Comparison of single-cell whole-genome amplification strategies

Nuria Estévez-Gómez[1,2,3#], Tamara Prieto[1,2,3#], Amy Guillaumet-Adkins[4,5§], Holger Heyn[4,5], Sonia Prado-López[1,2,3*] & David Posada[1,2,3*]

[1]Department of Biochemistry, Genetics and Immunology, University of Vigo, 36310 Vigo, Spain.

[2]Biomedical Research Center (CINBIO), University of Vigo, 36310 Vigo, Spain.

[3]Galicia Sur Health Research Institute, 36312 Vigo, Spain.

[4]CNAG-CRG, Centre for Genomic Regulation (CRG), Barcelona Institute of Science and Technology (BIST), Barcelona, Spain

[5]Universitat Pompeu Fabra (UPF), Barcelona, Spain

[#]Equal contributions

[§]Current address: Department of Pediatric Oncology, Dana Farber Cancer Institute, Harvard, 21 Medical School, Boston, MA 02115, USA.

*email: soniapradolopez@uvigo.es; dposada@uvigo.es

Single-cell genomics is an alluring area that holds the potential to change the way we understand cell populations. Due to the small amount of DNA within a single cell, whole-genome amplification becomes a mandatory step in many single-cell applications. Unfortunately, single-cell whole-genome amplification (scWGA) strategies suffer from several technical biases that complicate the posterior interpretation of the data. Here we compared the performance of six different scWGA methods (GenomiPhi, REPLIg, TruePrime, Ampli1, MALBAC, and PicoPLEX) after amplifying and low-pass sequencing the complete genome of 230 healthy/tumoral human cells. Overall, REPLIg outperformed competing methods regarding DNA yield, amplicon size, amplification breadth, amplification uniformity –being the only method with a random amplification bias–, and false single-nucleotide variant calls. On the other hand, non-MDA methods, and in particular Ampli1, showed less allelic imbalance and ADO, more reliable copy-number profiles and less chimeric amplicons. While no single scWGA method showed optimal performance for every aspect, they clearly have distinct advantages. Our results provide a convenient guide for selecting a scWGA method depending on the question of interest while revealing relevant weaknesses that should be considered during the analysis and interpretation of single-cell sequencing data.

30   Advances in single-cell genomics have made possible the study of genomic variation at the most basic

31   level, rapidly generating many new insights into complex biological systems, from microbial diversity

32   to immune response, development or tumor progression[1]. While single-cell RNA sequencing is now

33   mature and almost standard, single-cell DNA sequencing is still quite challenging[2], mainly due to an

34   amplification step needed before the characterization of the genome, as it is not possible to directly

35   sequence the 6-7 pg of DNA present, for example, in a human cell. While whole-genome single-cell

36   library preparation without preamplification is possible[3], these types of techniques still include several

37   PCR cycles, usually rely on custom-made microfluidic devices, and their implementation in a standard

38   laboratory is far from trivial. Therefore, single-cell whole-genome amplification (scWGA) is still a

39   prerequisite in many applications of single-cell genomics.

40   Multiple scWGA methods have been proposed, typically based on pure PCR[4–7], multiple

41   displacement amplification (MDA)[8,9] or a combination of both[10,11], but always relying on the use of

42   DNA polymerases. Unfortunately, the latter have a limited strand extension rate and processivity, and

43   during scWGA lots of priming and extension reactions are required[12]. This large amount of reactions

44   entails significant technical errors such as (1) allelic imbalance (AI) or allelic dropout (ADO) –when a

45   particular allele is preferentially amplified or not amplified at all, respectively–, (2) non-uniform

46   coverage usually attributed to GC content affecting denaturation and primer binding efficiency[13–15],

47   (3) generation of chimeric DNA molecules due to the polymerase strand displacement activity[16–18] and

48   (4) false single-nucleotide variants (SNVs) owing to the infidelity of the DNA polymerase[14] (Fig. 1).

49   While several studies comparing the relative performance of different scWGA strategies have

50   already been published, their scope is usually limited in terms of the sequencing target, number of

51   scWGA methods evaluated and/or number and type of amplified cells[16,17,19–30] (Supplementary Table

52   1). To date, we are not aware of any study comparing a large number of scWGA strategies on whole

53   genomes obtained from a large number of individual cells. Here we report a comprehensive

54   benchmark of six popular scWGA kits, including five next-generation sequencing (NGS) library

55   preparation kits and two NGS technologies, using three human cell lines. In total, we obtained 230

56   single-cell whole-genome sequences under 54 different scenarios (Fig. 2). We show that MDA and

57   non-MDA methods perform differently for distinct purposes, and identify important differences within

58   these categories. Our results should help single-cell genomics researchers choose the best

59   amplification method for their question of interest.

Results

61   We assessed the performance of six scWGA commercial kits, three MDA (GenomiPhi, REPLIg and

62   TruePrime) and three non-MDA (Ampli1, MALBAC and PicoPLEX) (Supplementary Table 2), and

five library preparation kits (Supplementary Table 3) in terms of amplification yield, amplicon size, coverage breadth, coverage uniformity, chimera formation, copy-number detection, allelic imbalance, ADO and false SNV detection. To do this, we obtained low-pass (0.07-1.8X) whole-genome sequencing (WGS) data from 230 individual human cells from a healthy fibroblast cell line (HDF), a colorectal cancer cell line (Caco-2), and a mantle lymphoma cell line (Z-138).

DNA yield, amplicon size, and integrity. The amount of DNA obtained with the different scWGA kits, plus the size and quality of the amplicons, could be a limitation for downstream experiments. Here, we observed statistically significant differences among the scWGA methods for DNA yield and amplicon integrity and size, independently of the cell line (Fig. 3 and Supplementary Tables 4-6). REPLIg resulted in the highest DNA yield by far with a mean value across cell lines close to 35 μg, while the other scWGA kits produced average yields below 8 μg (Fig. 3a and Supplementary Tables 4-6). MDA approaches (GenomiPhi, REPLIg, TruePrime) produced amplicon sizes much larger than non-MDA methods (Ampli1, MALBAC, PicoPLEX) (around 10 and 1.2 kb on average, respectively), with REPLIg producing the largest amplicons (>30 kb) (Fig. 3c and Supplementary Tables 4-6). The size of the amplicons produced by the MDA kits allowed us to estimate amplicon integrity using the DNA Integrity Number (DIN) value, with REPLIg showing significantly higher values than GenomiPhi or TruePrime (Fig. 3b and Supplementary Tables 5,6). For all these three parameters, MDA methods were much more variable than non-MDA approaches, in particular in the case of REPLIg, which displayed the largest standard deviations (Supplementary Tables 4-6).

Amplification breadth and uniformity. An ideal scWGA method should provide a set of DNA molecules that represent the target genome as completely as possible. If the amplification is not uniform, different genomic regions may be missed. Here, we observed statistically significant differences among scWGA methods for amplification breadth and uniformity for the different cell lines (Fig. 4a,b). Overall, REPLIg yielded the highest amplification breadth (~50%) and TruePrime the lowest (~15%) (Fig. 4a and Supplementary Tables 4-6). In general, REPLIg also resulted in a more uniform amplification –measured by the Gini index of the Lorenz curves– than the other scWGA methods, with TruePrime performing the worst (Fig. 4b; Supplementary Fig. 1 and Supplementary Tables 4-6). Again, MDA methods were much more variable than non-MDA approaches.

Albeit less dramatic, the library protocol also had a significant effect on amplification breadth and uniformity. Our modified KAPA protocol provided more breadth than the other library protocols, with Ion Plus being the worst in this aspect (Fig. 4c). Also, Ion Plus and Nextera yielded overall the most and least uniform amplifications, respectively (Fig. 4d). As expected, the two sequencing

3

96 technologies used, Illumina and Ion Torrent, did not have a significant effect on the uniformity of the
97 amplification. In order to better understand the joint effect of the different parameters (cell line,
98 scWGA kit, amplification location, library kit, yield DNA, amplicon size, sequencing depth and
99 sequencing technology) on amplification uniformity we fitted a multivariable regression model upon
100 the Gini index values, finding that differences in amplification uniformity could be explained by the
101 amplification kit alone.

102 **Amplification recurrence.** The coverage distribution along the genome observed for the single-cells
103 was significantly correlated with that of the unamplified bulk (Fig. 5). Importantly, we also found that
104 two cells amplified with the same scWGA kit showed significantly more regions in common than two
105 cells amplified with a different scWGA kit, except for REPLIg (Fig. 5 and Supplementary Figs. 2-4).
106 In addition, we observed that non-MDA showed a significantly higher coverage in regions with high
107 GC content, as previously reported[31]. Interestingly, REPLIg showed a negative correlation of coverage
108 with GC content whereas the other MDA methods did not show any preference based on sequence
109 content.

110 **Chimera rates, allelic imbalance, ADO and false SNVs.** During scWGA, several artifacts can be
111 produced, such as the formation of chimeric molecules, biased amplification of alleles, and
112 amplification errors. These errors can easily result in incorrect genotype calls. Here we measured
113 chimera rates, allelic imbalance, allelic dropout (ADO) and false positive variant calls (Fig. 6 and
114 Supplementary Table 7). In this case, only the HDF cell line (4 cells per scWGA method) was used as
115 it lacks somatic variation, which otherwise could have easily confounded these estimates. Chimera
116 rates were much higher (>10%) for GenomiPhi and TruePrime, with Ampli1 and MALBAC showing
117 the lowest values (Fig. 6a). When these rates were estimated upon paired-end discordant reads instead
118 of split reads, the trends were the same but the rates were twice as high (Fig. 6b).
119 In terms of allelic imbalance and ADO rates, non-MDA methods outperformed MDA
120 methods (Fig. 6c-e). Still, ADO rates were very high in all cases, ranging from the 38% rate of
121 Ampli1 to the 60-90% values observed for TruePrime. REPLIg, Ampli1, and TruePrime resulted in
122 more accurate SNV calls than the other methods (Fig. 6f,g), although the false positive rates obtained
123 were halved depending on the variant calling approach (marginal vs joint; see methods). False SNVs
124 were usually biased towards transitions, but different scWGA approaches showed somehow different
125 error signatures (Supplementary Fig. 5). In the case of Ampli1, these errors showed a pattern most
126 similar to the human germline mutational profile, in which transitions occur more than twice as often
127 as transversions. Besides, we also found an increase in G:C>A:T errors in REPLIg and GenomiPhi.

4

Copy-number detection. Copy number aberrations are a fundamental type of structural variation of interest to assess genomic heterogeneity among cells. The copy-number profiles estimated from the diploid HDF cell line were generally accurate (i.e., we expect a copy number of 2 for all genomic regions) for all scWGA methods, except for TruePrime (Supplementary Fig. 6d-i). The coverage dispersion measure (MAD)[32] was significantly smaller for non-MDA methods, although for Caco-2 REPLIg showed also very low MAD values (Supplementary Fig. 6a-c).

Mapping rates and duplicated reads. Finally, we explored the mapping rates and percentage of duplicated reads obtained. For all scWGA methods, we observed a high percentage of mapped reads (Supplementary Tables 4-6), with marginally significant differences among them (p-value = 0.04). In particular, TruePrime showed more reads mapped to the mitochondrial genome than the other scWGA kits (close to 9% in Caco-2, up to 6% in Z-138, and as high as 84.71% in HDF). Also, we detected clear mapping differences among the sequencing library kits (p-value < 2.2e-16). Within these, the library protocols that include an enrichment PCR step (SureSelect and Nextera) showed a significantly higher percentage of mapped reads (p-value = 3.8e-15). Additionally, we found a clear effect of the sequencing technology on the percentage of duplicates estimated, with Ion Torrent producing significantly more duplicates than Illumina (24% and 6%, respectively; p-value < 2.2e-16).

Benchmark of the breadth and uniformity measures. As an estimate of amplification breadth, we used low-pass sequencing data to predict the fraction of the genome covered at higher sequencing depths with the package Preseq[33]. To evaluate amplification uniformity, we used the Gini index or area below the coverage Lorenz curve. To validate both measurements we leveraged an *in-house* dataset of 30 single cells from a Chronic Lymphocytic Leukemia (CLL) patient. The analysis of these data demonstrated that the amplification breadth prediction was very accurate (Supplementary Fig. 7). In addition, both the breadth prediction and the 1 – Gini index showed a significant positive correlation with the percentage of chromosomes amplified (Supplementary Fig. 8).

Discussion

Overall, our results show that MDA approaches (GenomiPhi, REPLIg, TruePrime) produced higher yields than non-MDA methods (Ampli1, MALBAC, PicoPLEX), which could be related to a more stable polymerase activity under isothermal conditions[34]. At the same time, MDA approaches generated larger amplicon sizes than non-MDA methods, likely due to a higher processing capability and template affinity of the Phi29 polymerase[35]. In particular, REPLIg clearly outperformed the other scWGA strategies in this aspect, possibly resulting from a higher DNA polymerase concentration[36].

159 TruePrime resulted in a significantly lower coverage breadth, as previously reported[28], with

160 REPLIg outperforming the remaining methods in general, but with higher variance, as the other MDA

161 methods. This might be explained, at least partially, by the random annealing of primers and/or more

162 variable amplicon sizes of the MDA methods. In agreement with the coverage breadth predictions,

163 REPLIg and TruePrime resulted in the most and least uniform amplifications, respectively, measured

164 by the variation of the coverage along the genome. The lysis and denaturalization steps in TruePrime

165 are made on ice, which might prevent the availability of single-stranded DNA for the primase. On the

166 other hand, REPLIg has already been suggested to provide a more uniform coverage than non-MDA

167 methods for few-cell amplification[30].

168 The observed coverage correlation along the genome between single cells and the unamplified

169 bulk was expected, mainly due to mappability limitations for repetitive sequences[37]. However, unless

170 there is a recurrent amplification bias, we would not expect to see higher correlations among cells

171 amplified with the same scWGA kit compared to cells amplified with a different scWGA kit, or

172 compared with the bulk. Therefore, our results suggest that the amplification bias along the genome is

173 not random for the different scWGA kits studied, except for REPLIg, which in most cases resulted in

174 apparently random amplification. For non-MDA methods, spatial recurrence in the amplification is

175 expected because they use their own set of non-random primers. For MDA methods, the results are

176 more difficult to interpret. TruePrime uses a primase that generates its own primers[9], while for both

177 GenomiPhi and REPLIg random primers are added. However, only REPLIg showed a random

178 amplification bias. Zhang et al.[12] obtained a better fit with a statistical model with random

179 amplification bias for MDA, but they do not clarify which exact MDA method they used.

180 For the HDF cell line, non-MDA methods showed a distribution more similar to the bulk for

181 the alternative allele frequency in heterozygous germline sites, clearly outperforming the MDA

182 methods in terms of allelic imbalance. In particular, Ampli1 seemed to produce very low allelic

183 imbalance. This good behavior of Ampli1 might be the result of a synthesis procedure that converts

184 residual single-strand DNA (ssDNA) molecules into double-strand DNA (dsDNA) molecules. Also, in

185 PicoPLEX and MALBAC the amplification is quasi-linear, therefore limiting the propagation of any

186 allelic bias. We would like to remark that, in general, alternative allele frequency distributions are

187 wider for our single cells than for the bulk not only because of allelic imbalance but also because they

188 have lower coverage at the sites considered.

189 In agreement with these results –ADO is an extreme case of allelic imbalance–, non-MDA

190 methods showed much lower ADO rates than MDA methods, in particular Ampli1, who showed the

191 lowest ADO rate (< 40%). On the other extreme, TruePrime showed a large ADO rate (> 80%). Still,

192 a 40% ADO rate is much higher than previously reported for Ampli1[25,38,39]. Although values over 40%

193 have been already observed in other experiments for MDA methods[40], here the ADO rates for

GenomiPhi and REPLIg were closer to 60%. Admittedly, it is possible that the absolute ADO values estimated here are somehow inflated due to the small coverage. It is well-known that at sites with low coverage there is a higher probability of missing one of the alleles by chance[41]. Although we have carried out this analysis on sites with at least 6X, we are aware that at this depth it is possible to incorrectly call as homozygous a truly heterozygous site. Indeed, genotyping of heterozygous sites only approximates a correct call rate of 1.0 for coverages higher than 15X[42], although a threshold value of 6X has been used before to estimate ADO and false SNV rate[40]. In any case, the relative ADO performance should still correspond with the trend observed.

We used false SNVs as proxies for amplification errors. Indeed, the former also include sequencing errors, wrong SNV calls and potentially some true somatic variants, so the absolute value might be more or less inflated. However, the comparison of the false SNVs observed for each scWGA method should inform us about their relative amplification error rates. We used a PCR-free library protocol, and sequencing errors should be similar for all 24 HDF single-cell libraries, as they were included in the same sequencing run. Also, most of the true somatic variants should have been filtered out with the help of Monovar. Finally, whatever it is, the number of calling errors should be more or less constant across cells. REPLIg and TruePrime resulted in the lowest false SNV rates (< 8% depending on the genotyping approach). This might be related to the polymerase used for amplification, Phi29, which has a much lower error rate than the ones used by the other scWGA kits[8,10,11,14,43–45]. REPLIg was already reported as having low error rates[17,28]. Ampli1 also performed quite well in this regard, perhaps due to the use of a combination of Taq with a proofreading polymerase Pwo[7] with low error rates[46]. Importantly, when we used joint variant calling –incorporating population-level information–, the inferred false positive rates were halved. With regard to the type of errors observed, we found that both REPLIg and GenomiPhi resulted in an excess of C:G>T:A transitions, which has been previously attributed to high-temperature denaturation protocols, whereas the signature for Ampli1 better reflects the one expected for unamplified bulk samples[47]. Being aware of the existence of a different error signature for the different scWGA kits is a fact to consider if one is interested in detecting mutational signatures in single cells.

Our results suggest that MALBAC and Ampli1 form fewer chimeras than the other methods. Indeed, chimeras can bias the inference of structural variants. It was expected for MDA methods to perform worse than non-MDA methods in this regard, due to the Phi29 DNA polymerase strand displacement activity resulting in chimeric molecules[18]. However, despite the fact that REPLIg is based on MDA, it showed very low chimera rates, even lower than microfluidic protocols[48]. Perhaps, this might be related to larger amounts of DNA polymerase which could limit the time that ssDNA strands are naked and available for chimera formation.

228   For the HDF cell line, copy-number profiles were in general accurate for all scWGA methods

229   except for TruePrime. In the other cell lines, the copy-number profiles were much more segmented.

230   Nevertheless, read counts were much more dispersed for MDA methods (except for REPLIg in the

231   HDF cell line), which could be partially explained by uneven amplification (Supplementary Fig.

232   6a-c). Consequently, non-MDA methods would be the recommended choice for CNV analysis, as

233   suggested before[11,38].

234   Not surprisingly, the amplification protocols did not significantly affect the mapping rates.

235   While the scWGA kit employed had a much smaller effect on the percentage of mapped reads than the

236   library construction method –strategies with an enrichment PCR step like SureSelect and Nextera

237   were better–, in all cases these percentages were quite high. As expected, probably due to the

238   emulsion PCR step[49] included in the Ion Torrent sequencing protocol, the latter showed significantly

239   more duplicates than Illumina.

240   In conclusion, none of the scWGA methods outperformed the others in all scenarios assessed,

241   but clearly, some are better than others in different aspects. Here we have exposed distinct advantages

242   and weaknesses of different scWGA methods that will be important for the interpretation and analysis

243   of single-cell genomes.

Methods

244

245   **Cell-lines.** We used three different cell lines for the different experiments, HDF, Caco-2, and Z-138.

246   HDF is a healthy neonatal, diploid fibroblast cell line (HDF) purchased from Sigma-Aldrich

247   (https://www.sigmaaldrich.com). Caco-2 is a polyploid colorectal cancer cell line with a modal

248   chromosome number of 96 purchased from the American Type Culture Collection (ATCC;

249   https://www.atcc.org). The Z-138 is a hyperdiploid mantle cell lymphoma cell line with a modal

250   chromosomal number of 49, also purchased from ATCC. We cultured all cell lines under an

251   atmosphere containing 5% CO_2 at 37℃. We grew HDF in an all-in-one ready-to-use fibroblast growth

252   media (Sigma-Aldrich), Caco-2 in a media consisting of Dulbecco's Modified Eagle's Medium/F12

253   with 3.151 g/l glucose and L-glutamine (Lonza) and Z-138 with Iscove's Modified Dulbecco's

254   Medium (ATCC). For Caco-2 and Z-138, we completed the media with 10% fetal bovine serum EU

255   standard (Biochrom) and 1% penicillin/streptomycin (Lonza) at a working concentration of 100 units

256   of potassium penicillin and 100 μg of streptomycin sulfate per 1 ml of culture media.

257   **Single-cell isolation.** We cultured HDF and Caco-2 cells until 80% confluence before staining with

258   Hoechst 33342 (BD Biosciences) following the fabricant's recommendations. Thereafter, we

259   harvested, resuspended at a concentration of 10^6 cells per ml in phosphate buffered saline (PBS) and

marked cells with propidium iodide (PI; BD Pharmingen). Then, we sorted live single cells in G0/G1 with a BD Biosciences FACSAria III flow cytometer (BD Biosciences, Madrid, Spain) and collected them into 96 well plates with 1-3 µl of PBS (Supplementary Fig. 9). For sorting, we used the BD FACSDiva v8.0.1 (BD Biosciences, Madrid, Spain) and FlowJo v7.6.2 (FlowJo, LLC, Ashland, OR, USA) for further analyses. For Z-138 we followed the same strategy but without Hoechst staining and using a FACS Aria 2.0 (BD Biosciences, Madrid, Spain) for sorting. Single cells were stored at -80 ºC until amplification.

Single-cell whole-genome amplification. We used six different kits for single-cell whole-genome amplification (scWGA): Ampli1 (Silicon Biosystems), Multiple Annealing and Looping Based Amplification Cycles (MALBAC; Yukon Genomics), PicoPLEX (Rubicon Genomics), Illustra Single Cell GenomiPhi (GE Healthcare), REPLIg Single-Cell (Qiagen) and TruePrime (SYGNIS) following the manufacturer's protocols (Supplementary Table 2). In order to reduce contamination, we carried out scWGA in a laminar-flow hood using a dedicated set of pipettes and UV irradiated plastic materials. We also included positive (10 ng/µl REPLIg human control kit, QIAGEN) and negative (DNase/RNase free water) controls. For Ampli1 we carried a few extra steps after amplification. We used the Ampli1 QC kit to select those amplification products that were positive for four PCR markers. In order to increase the total dsDNA content, we used the Ampli1 ReAmp/ds kit. Afterwards, we removed the adaptors adding 5 µl of NEBuffer 4 10X (New England Biolabs), 1 µl of MseI 50U/µl (New England Biolabs) and 19 µl of nuclease-free water to 25 µl of dsDNA, using a thermal cycler at 37 ºC for 3 h, followed by enzyme inactivation at 65 ºC for 20 min.

Attending to the fabricant's recommendations, we purified PicoPLEX and MALBAC products with the QIAquick PCR Purification protocol (Qiagen) and Ampli1 products with 1.8X AMPure XP beads (Agencourt, Beckman Coulter). MDA methods do not include a purification step. We measured DNA yield with a Qubit 3.0 (ThermoFisher Scientific) fluorometer and amplicon fragment size with a 2200 TapeStation platform (Agilent Technologies). We measured amplicons from non-MDA based scWGA methods using the D5000 ScreenTape System and amplicons from MDA-based kits using the Genomic DNA ScreenTape System. The latter also allowed us to measure the integrity of the amplicons (DNA Integrity Number or DIN).

In total, we amplified 230 single-cells: 34 with Ampli1 (4 HDF, 12 Caco-2 and 18 Z-138), 40 with MALBAC (4 HDF, 18 Caco-2 and 18 Z-138), 40 with PicoPLEX (4 HDF, 18 Caco-2 and 18 Z-138), 37 with GenomiPhi (4 HDF, 18 Caco-2 and 15 Z-138), 35 with REPLIg (4 HDF, 16 Caco-2 and 15 Z-138) and 44 with TruePrime (4 HDF, 22 Caco-2 and 18 Z-138) (Fig. 2 and Supplementary Table 2).

293   **Bulk DNA extraction.** We extracted bulk genomic DNA (gDNA) from the HDF cell line with the

294   QIAamp DNA Mini kit (QIAGEN) according to the fabricant's recommendations. We estimated

295   concentration and gDNA integrity as previously described for single cells.

296   **Next-generation sequencing libraries.** We built 230 single-cell whole-genome libraries employing

297   five different library preparation kits: SureSelect^{QXT} (Agilent Technologies), NxSeq AmpFREE Low

298   DNA (Lucigen), Ion Plus Fragment library (ThermoFisher Scientific), Nextera DNA (Illumina) and

299   KAPA (Kapa Biosystems). We built SureSelect and NxSeq libraries following the commercial

300   indications while we slightly modified Ion Plus and Nextera. The sequencing facility of the National

301   Center for Genomic Analysis (CNAG; http://www.cnag.crg.eu) modified the KAPA protocol to a

302   larger extent (Supplementary Table 3). We mechanically sheared the DNA in an S2 or a LE220

303   Focused-ultrasonicator (Covaris) for the NxSeq, Ion Plus and KAPA protocols (Supplementary Table

304   8), while for SureSelect and Nextera we fragmented the DNA enzymatically. For Ion Plus, we

305   included an extra purification step with AMPure XP beads (1.2X beads/sample ratio) (Agencourt,

306   Beckman Coulter) for a better removal of NGS adaptors. For Nextera, we used 200 µl of washing

307   buffer instead of the 300 µl recommended by the provider, the centrifugation speed was 10,000 g at

308   room temperature (RT) for 30 s instead of 1,300 g at 20 ºC for 2 min, and we used AMPure XP beads

309   in a 0.8X ratio instead of 0.6X. In addition, we eluted the Nextera libraries in 20 µl of resuspension

310   buffer instead of 32.5 after a 5 min air-dried step instead of 15. For the modified KAPA protocol, we

311   carried out the end-repaired of 500 ng of sheared DNA, adenylation and ligation to Illumina specific

312   indexed paired-end adaptors (NEXTflex-96™ DNA Barcodes, Bio Scientific). We performed the

313   DNA size selection in two steps (0.65X and 0.85X beads/sample ratio) with AMPure XP beads in

314   order to reach the desired fragment size (450 bp). Finally, we measured library insert sizes with a 2100

315   Bioanalyzer High Sensitivity DNA Kit (Illumina) or a 2200 TapeStation High Sensitivity D1000 (Ion

316   Torrent). We quantified library concentration with the Kapa Library Quantification Kit (Kapa

317   Biosystems) for Illumina and the Ion Library Quantitation Kit (Life Technologies) for Ion Torrent.

318   In addition, we constructed a whole-genome HDF bulk library using NxSeq AmpFREE Low

319   DNA (Lucigen) (Supplementary Table 3). We performed size selection using AMPure XP beads and

320   we checked fragments size with the 2100 Bioanalyzer High Sensitivity DNA Kit. Finally, we

321   quantified library concentration using the KAPA Library Quantification Kit.

322   **Whole-genome sequencing.** We sequenced single-cell libraries at shallow depths (0.07-1.76X). We

323   sequenced 24 HDF and 166 Caco-2/Z-138 libraries on an Illumina HiSeq 4000 (PE150) or HiSeq

324   2000 (PE125), respectively, at CNAG. We sequenced the remaining 40 libraries with an Ion Proton

325   platform (Ion PI chip v3) at the Galician Public Foundation of Genomic Medicine (FPGMX;

326   http://www.xenomica.eu). We sequenced the bulk library of HDF at 30X on an Illumina HiSeq 4000

327   (PE150) at CNAG.

328   **Preprocessing of NGS data.** We clipped library adapters and also those included in the Ampli1,

329   PicoPLEX and MALBAC amplifications using CutAdapt (v.1.11,v.1.14)[50]. We mapped the sequencing

330   reads with at least 70 bp to the human reference genome (hs37d5) with BWA-MEM

331   (v.0.7.15-r1140)[51]. We sorted reads and flagged duplicates with Picard *SortSam* (v.2.2.1;

332   http://broadinstitute.github.io/picard) and Picard *MarkDuplicates*, respectively. We independently

333   mapped reads from different lanes and then merged during the duplicate marking process taking into

334   account their read group. Regarding Ion Plus libraries, the sequencer software already removed the

335   adapters. In order to map the reads with the Torrent Mapping Alignment Program (TMAP; v.3.4.1;

336   https://github.com/iontorrent/TMAP) to the hs37d5 genome, we had to transform first of all the

337   original BAM files to FASTQ format using Picard *SamToFastq*. We also sorted the BAM files and

338   marked duplicates as explained above.

339   For the 24 HDF single-cells and bulk, which were subsequently used for variant calling, the base

340   quality scores were recalibrated for each sample using GATK (v.3.7)[52]. Afterward, we realigned reads

341   from the single-cells and bulk together around known indels to avoid potential false SNV calls not

342   related to the amplification process itself but due to misalignments.

343   **Amplification breadth.** In order to approximate the amplification breadth, we calculated the

344   percentage of the genome that would be covered by one or more reads (coverage breadth). However,

345   we did not calculate this value directly because at very low depths this estimate is not reliable due to

346   sampling error[12]. Instead, we used a method developed for single-cell libraries, implemented in the

347   *gc_extrap* function of the package Preseq[33]. For this calculation, we downsampled the BAM files to

348   the lowest depth observed (0.07X) with Picard *DownsampleSam*. To check the quality of the Preseq

349   prediction, we took advantage of two *in-house* datasets consisting of 30 single-cells from a patient

350   with Chronic Lymphocytic Leukemia (CLL), that were amplified with REPLIg and sequenced twice

351   at 0.3X-0.6X and 5X. We downsampled the former to exactly 0.1X and predicted with Preseq the

352   percentage of the genome covered by one or more reads at 5X. Then, we compared this prediction

353   with the values observed for the 5X dataset. In addition, we compared the Preseq prediction and the

354   Gini index (see below) with the percentage of chromosomes amplified in the same 30 CLL single

355   cells, according to a panel of 20 PCR markers representing all human chromosomes except 6 and 11.

356   **Amplification uniformity**. We used coverage uniformity as a surrogate for amplification uniformity.

357   For this, we used the downsampled BAM files at 0.07X. We calculated the sequencing depth per site

11

358   with Bedtools[53] and parsed its output with an *in-house* script to create the Lorenz curves[47] with the *Lc*

359   function of the *Ineq* R package. In order to quantitatively compare the Lorenz curves, we calculated

360   the Gini index for each cell[20]. The Gini index measures the area below the Lorenz curve, spanning

361   between 0 and 1, being 0 perfect uniformity and 1 perfect disuniformity, so we defined amplification

362   uniformity as 1 minus the Gini index (see also Supplementary Fig. 1). We estimated the Gini indexes

363   using the *Gini* function from the *Ineq* package. In order to understand which variables of the study

364   (cell line, scWGA kit, amplification location, library kit, DNA yield, amplicon size, sequencing depth

365   and sequencing technology) affect most the Gini index, we fitted a regression model.

366   **Amplification recurrence.** In order to understand whether a given scWGA method tends to

367   preferentially amplify the same genomic regions in different cells compared to other scWGA methods,

368   we counted the number of reads within non-overlapping windows of 1 Mb with Pysamstats

369   (https://github.com/alimanfoo/pysamstats). For this, we used downsampled BAM files at 0.1X –after

370   removing duplicates, secondary alignments and unmapped reads with Samtools *view*[54]– as input. We

371   only used the HDF cell line for this calculation in order to avoid potential correlations among read

372   counts due to a heterogeneous copy number in the cancer cell lines. Subsequently, we computed the

373   Pearson correlation coefficient of the read counts between pairs of single-cells (amplified with the

374   same scWGA kit or not) and between single-cell and bulk. We further explored the correlations

375   between read counts and GC content in sliding windows. GC content was assessed with Bedtools *nuc*.

376   However, since having for instance 2 reads of 150 bp mapped to the same 1 Mb window in two

377   different single-cells does not necessarily mean that they amplify exactly the same region (in one cell

378   reads could be mapped to the first 500 bp of the window and in the other cell to the last 500), we

379   further explored presence/absence amplification recurrences computing Jaccard similarity

380   coefficients. For this, we created bedGraph files for each of the single cells using Bedtools

381   *genomecov*, simplified integer coverage values simply to 1 (presence) or 0 (absence) and then merged

382   the resulting files using Bedtools *unionbedg* to get a matrix. We removed consecutive matrix rows

383   which showed exactly the same presence/absence profile for the 24 HDF cells, as we wanted to be

384   stringent and do not count several events from a single read recurrence. Then, we computed the

385   Jaccard similarity coefficient for each pair of single-cells using the R package *jaccard*

386   (https://cran.r-project.org/web/packages/jaccard/index.html). Basically, the Jaccard coefficient is

387   computed by dividing the number of intersections (presence of coverage in both cells) between the

388   number of total unions (presence of coverage in just one cell), this way ignoring positions without

389   coverage for the two cells (avoiding increasing the similarity due to random absence of coverage

390   originated by low pass sequencing). To assess its statistical significance, we implemented a

391   permutation test using a homemade R script.

392 **Chimera formation rate.** We considered the paired-end reads mapping at a distance higher than 1 kb
393 to result from chimeric amplicons, as well as reads with supplementary alignments (split reads). We
394 calculated paired-end distances using Picard *CollectAlignmentSummaryMetric* and identified split
395 reads through detection of SA:Z tags in the BAM files. For this calculation, we only used the HDF
396 cell line in order to avoid false positives due to the high genetic instability in Caco-2 and Z-138.

397 **Allelic imbalance and ADO.** During scWGA, the two alleles of a diploid single-cell can be amplified
398 in an unequal manner. Deviations of allele frequencies at heterozygous germline sites evince such
399 events. If these frequencies are different from the theoretical 50%, we consider that an allelic
400 imbalance event, and if the deviation is so high that one of the alleles is completely lost and it cannot
401 be detected, we designate it as ADO (Fig. 1). Again, for these calculations, we only used the HDF
402 cells, as Caco-2 and Z-138 cells present variable ploidy.

403 *Allelic imbalance.* We ran GATK *HaplotypeCaller* for the HDF bulk with the parameter
404 --pcr_indel_model set to NONE. We used GATK *SelectVariants* to keep the heterozygous sites and
405 ran GATK *VariantRecalibration* (v. 4.0.0.0) to select a high confidence set. In parallel, we created
406 pileup files from all the HDF single-cells and bulk with Samtools *mpileup* and extracted the
407 alternative allele fraction at the high confidence heterozygous positions using a Python script
408 (Supplementary Information). We only considered the allele frequencies derived from sites covered by
409 at least six reads. In order to obtain a smooth distribution from the discrete counts, we estimated the
410 probability density function of the alternative allele fractions with the *core* R stats package, with the
411 *bandwidth adjust* parameter set to three.

412 *Allelic dropout (ADO).* In order to measure ADO, we first had to obtain genotypes both for the bulk
413 and the single cells. For this, we ran GATK *HaplotypeCaller* in ERC mode for all HDF single-cells
414 and bulk independently (for the latter again setting --pcr_indel_model to NONE) and merged the
415 results using two different approaches with GATK *GenotypeGVCF*. On one hand, we aggregated the
416 bulk and the 24 single-cells ("*joint calling*") and on the other hand, we simply combined one
417 single-cell and the bulk one at a time ("*marginal calling*"). We counted an ADO event when the bulk
418 was genotyped as heterozygous (AB) and the single-cell as homozygous for either the reference or the
419 alternative allele (AA or BB) (Supplementary Fig. 10). For this calculation, we only considered
420 positions covered by six or more reads in single cells and 15 or more reads in the bulk.

421 **Amplification polymerase errors**. We used false SNV calls ("false positives" or FP) as proxies for

13

422 amplification errors of the polymerase. Using the same genotypes estimated above for the ADO

423 calculation, we counted an FP event when the bulk genotype was homozygous (AA or BB) and the

424 single cell heterozygous (AB) (Supplementary Fig. 10). However, given the high number of somatic

425 mutations expected to accumulate during cell growth on a plate and with the intention of mitigating

426 their effect on the calculation of the FP rate, we did not consider for this calculation SNVs detected by

427 the single-cell variant caller MonoVar[55], nor sites with two or more reads containing the "potentially

428 erroneous allele" in the bulk. That is, we preferred not to be very stringent and allowed one error in

429 the bulk potentially arising by a sequencing or mapping error. Again, we only considered positions

430 with six or more reads for single cells and 15 or more reads for the bulk. We also explored the

431 mutational profile (signature) of the FPs directly extracting alternative and reference alleles from the

432 marginal calling VCFs and grouped them into different categories.

433 **Copy-number detection.** The uneven distribution of the coverage, added to the existence of ADO,

434 can make copy number detection from single-cell problematic. We compared how different scWGA

435 kits behave in this regard using the coverage dispersion measure (MAD) explained in Garvin et al.[32].

436 For this calculation, we used the downsampled BAM files at the lowest depth for each cell line

437 (0.25X, 0.07X, and 0.08X for HDF, Caco-2 and Z-138, respectively). We filtered out reads with a

438 mapping quality lower than 20 from the downsampled BAMs using Samtools and created with

439 Bedtools the BED files required to run Ginkgo[32]. We ran Ginkgo under default settings except for the

440 Binning Simulation Options that were set to 150 bp reads and BWA mapping. The segmentation was

441 inferred independently for each sample to allow a fair comparison.

442 **Statistical tests.** We calculated descriptive statistics using the *kruskal.test*, *wilcox.test*, and *cor.test*

443 functions available in the *core* R stats package[56]. For the regression models, we used the R package

444 *FWDselect*[57].

Code availability

446 The R and bash scripts used for this study are available as Supplementary Information.

Data availability

448 Bulk and single-cell FASTQ files generated for this study have been deposited at the Sequence Read

449 Archive (SRA) under STUDY accession SRP162960.

14

Acknowledgments

Author contributions

N.E.-G., S.P.-L., A.G.-A. and H.H. performed the experiments. T.P. carried out the bioinformatic analyses. N.E.-G. and T.P. performed the statistical analyses. N.E.-G., T.P., S.P., and D.P. wrote the manuscript. All authors read, commented and approved the final manuscript. D.P. designed the project and supervised the whole study.

Competing interests

The authors declare no competing interests.

References

1. Gawad, C., Koh, W. & Quake, S. R. Single-cell genome sequencing: current state of the science. *Nat. Rev. Genet.* **17,** 175–188 (2016).
2. Linnarsson, S. & Teichmann, S. A. Single-cell genomics: coming of age. *Genome Biol.* **17,** 97 (2016).
3. Zahn, H. *et al.* Scalable whole-genome single-cell library preparation without preamplification. *Nat. Methods* **14,** 167–173 (2017).
4. Nelson, D. L. *et al.* Alu polymerase chain reaction: a method for rapid isolation of human-specific sequences from complex DNA sources. *Proc. Natl. Acad. Sci. U. S. A.* **86,**

483   6686–6690 (1989).

484   5. Zhang, L. *et al.* Whole genome amplification from a single cell: implications for genetic analysis.
485   *Proc. Natl. Acad. Sci. U. S. A.* **89,** 5847–5851 (1992).

486   6. Telenius, H. *et al.* Degenerate oligonucleotide-primed PCR: general amplification of target DNA
487   by a single degenerate primer. *Genomics* **13,** 718–725 (1992).

488   7. Klein, C. A. *et al.* Comparative genomic hybridization, loss of heterozygosity, and DNA
489   sequence analysis of single cells. *Proceedings of the National Academy of Sciences* **96,**
490   4494–4499 (1999).

491   8. Dean, F. B. *et al.* Comprehensive human genome amplification using multiple displacement
492   amplification. *Proc. Natl. Acad. Sci. U. S. A.* **99,** 5261–5266 (2002).

493   9. Picher, Á. J. *et al.* TruePrime is a novel method for whole-genome amplification from single cells
494   based on TthPrimPol. *Nat. Commun.* **7,** 13296 (2016).

495   10. Kamberov, E. *et al.* Amplification and analysis of whole genome and whole transcriptome
496   libraries generated by a DNA polymerization process. *US Patent* (2012).

497   11. Zong, C., Lu, S., Chapman, A. R. & Xie, X. S. Genome-wide detection of single-nucleotide and
498   copy-number variations of a single human cell. *Science* **338,** 1622–1626 (2012).

499   12. Zhang, C.-Z. *et al.* Calibrating genomic and allelic coverage bias in single-cell sequencing. *Nat.*
500   *Commun.* **6,** 6822 (2015).

501   13. Hou, Y. *et al.* Single-cell exome sequencing and monoclonal evolution of a JAK2-negative
502   myeloproliferative neoplasm. *Cell* **148,** 873–885 (2012).

503   14. Navin, N. E. Cancer genomics: one cell at a time. *Genome Biol.* **15,** 452 (2014).

504   15. Sabina, J. & Leamon, J. H. Bias in Whole Genome Amplification: Causes and Considerations.
505   *Methods Mol. Biol.* **1347,** 15–41 (2015).

506   16. Voet, T. *et al.* Single-cell paired-end genome sequencing reveals structural variation per cell
507   cycle. *Nucleic Acids Res.* **41,** 6119–6138 (2013).

508   17. Huang, L., Ma, F., Chapman, A., Lu, S. & Xie, X. S. Single-Cell Whole-Genome Amplification
509   and Sequencing: Methodology and Applications. *Annu. Rev. Genomics Hum. Genet.* **16,** 79–102
510   (2015).

511   18. Lasken, R. S. & Stockwell, T. B. Mechanism of chimera formation during the Multiple
512   Displacement Amplification reaction. *BMC Biotechnol.* **7,** 19 (2007).

513   19. Chen, M. *et al.* Comparison of multiple displacement amplification (MDA) and multiple
514   annealing and looping-based amplification cycles (MALBAC) in single-cell sequencing. *PLoS*
515   *One* **9,** e114520 (2014).

516   20. de Bourcy, C. F. A. *et al.* A Quantitative Comparison of Single-Cell Whole Genome
517   Amplification Methods. *PLoS One* **9,** e105585 (2014).

518   21. Ning, L. *et al.* Quantitative assessment of single-cell whole genome amplification methods for
519   detecting copy number variation using hippocampal neurons. *Sci. Rep.* **5,** 11415 (2015).

520   22. Hou, Y. *et al.* Comparison of variations detection between whole-genome amplification methods
521   used in single-cell resequencing. *Gigascience* **4,** 37 (2015).

522   23. Li, N. *et al.* The Performance of Whole Genome Amplification Methods and Next-Generation
523   Sequencing for Pre-Implantation Genetic Diagnosis of Chromosomal Abnormalities. *J. Genet.*
524   *Genomics* **42,** 151–159 (2015).

525   24. Deleye, L. *et al.* Whole genome amplification with SurePlex results in better copy number
526   alteration detection using sequencing data compared to the MALBAC method. *Sci. Rep.* **5,** 11711
527   (2015).

528   25. Babayan, A. *et al.* Comparative study of whole genome amplification and next generation

16

529   sequencing performance of single cancer cells. *Oncotarget* **8,** 56066–56080 (2016).

530   26. Deleye, L. *et al.* Performance of a TthPrimPol-based whole genome amplification kit for copy
531   number alteration detection using massively parallel sequencing. *Sci. Rep.* **6,** 31825 (2016).

532   27. Deleye, L. *et al.* Performance of four modern whole genome amplification methods for copy
533   number variant detection in single cells. *Sci. Rep.* **7,** 3422 (2017).

534   28. Biezuner, T. *et al.* Comparison of seven single cell Whole Genome Amplification commercial
535   kits using targeted sequencing. Preprint at
536   https://www.biorxiv.org/content/early/2017/09/11/186940 (2017).

537   29. Borgström, E., Paterlini, M., Mold, J. E., Frisen, J. & Lundeberg, J. Comparison of whole
538   genome amplification techniques for human single cell exome sequencing. *PLoS One* **12,**
539   e0171566 (2017).

540   30. Deleye, L., Gansemans, Y., De Coninck, D., Van Nieuwerburgh, F. & Deforce, D. Massively
541   parallel sequencing of micro-manipulated cells targeting a comprehensive panel of
542   disease-causing genes: A comparative evaluation of upstream whole-genome amplification
543   methods. *PLoS One* **13,** e0196334 (2018).

544   31. Benjamini, Y. & Speed, T. P. Summarizing and correcting the GC content bias in high-throughput
545   sequencing. *Nucleic Acids Res.* **40,** e72 (2012).

546   32. Garvin, T. *et al.* Interactive analysis and assessment of single-cell copy-number variations. *Nat.*
547   *Methods* **12,** 1058–1060 (2015).

548   33. Daley, T. & Smith, A. D. Modeling genome coverage in single-cell sequencing. *Bioinformatics*
549   **30,** 3159–3165 (2014).

550   34. Pinard, R. *et al.* Assessment of whole genome amplification-induced bias through
551   high-throughput, massively parallel whole genome sequencing. *BMC Genomics* **7,** 216 (2006).

552   35. Blanco, L. *et al.* Highly efficient DNA synthesis by the phage phi 29 DNA polymerase.
553   Symmetrical mode of DNA replication. *J. Biol. Chem.* **264,** 8935–8940 (1989).

554   36. Dimitriadou, E., Zamani Esteki, M. & Vermeesch, J. R. Copy Number Variation Analysis by
555   Array Analysis of Single Cells Following Whole Genome Amplification. *Methods Mol. Biol.*
556   **1347,** 197–219 (2015).

557   37. Treangen, T. J. & Salzberg, S. L. Repetitive DNA and next-generation sequencing: computational
558   challenges and solutions. *Nat. Rev. Genet.* **13,** 36–46 (2011).

559   38. Binder, V. *et al.* A New Workflow for Whole-Genome Sequencing of Single Human Cells. *Hum.*
560   *Mutat.* **35,** 1260–1270 (2014).

561   39. Normand, E. *et al.* Comparison of three whole genome amplification methods for detection of
562   genomic aberrations in single cells. *Prenat. Diagn.* **36,** 823–830 (2016).

563   40. Leung, M. L., Wang, Y., Waters, J. & Navin, N. E. SNES: single nucleus exome sequencing.
564   *Genome Biol.* **16,** 55 (2015).

565   41. Nielsen, R., Paul, J. S., Albrechtsen, A. & Song, Y. S. Genotype and SNP calling from
566   next-generation sequencing data. *Nat. Rev. Genet.* **12,** 443–451 (2011).

567   42. Maruki, T. & Lynch, M. Genotype Calling from Population-Genomic Sequencing Data. *G3* **7,**
568   1393–1404 (2017).

569   43. Esteban, J. A., Salas, M. & Blanco, L. Fidelity of phi 29 DNA polymerase. Comparison between
570   protein-primed initiation and DNA polymerization. *J. Biol. Chem.* **268,** 2719–2726 (1993).

571   44. Paez, J. G. *et al.* Genome coverage and sequence fidelity of 29 polymerase-based multiple strand
572   displacement whole genome amplification. *Nucleic Acids Res.* **32,** e71–e71 (2004).

573   45. Keohavong, P. & Thilly, W. G. Fidelity of DNA polymerases in DNA amplification. *Proc. Natl.*
574   *Acad. Sci. U. S. A.* **86,** 9253–9257 (1989).

46. McInerney, P., Adams, P. & Hadi, M. Z. Error Rate Comparison during Polymerase Chain Reaction by DNA Polymerase. *Mol. Biol. Int.* **2014,** 287430 (2014).

47. Dong, X. *et al.* Accurate identification of single-nucleotide variants in whole-genome-amplified single cells. *Nat. Methods* **14,** 491–493 (2017).

48. Hosokawa, M., Nishikawa, Y., Kogawa, M. & Takeyama, H. Massively parallel whole genome amplification for single-cell sequencing using droplet microfluidics. *Sci. Rep.* **7,** 5199 (2017).

49. Balzer, S., Malde, K., Grohme, M. A. & Jonassen, I. Filtering duplicate reads from 454 pyrosequencing data. *Bioinformatics* **29,** 830–836 (2013).

50. Martin, M. Cutadapt removes adapter sequences from high-throughput sequencing reads. *EMBnet.journal* **17,** 10 (2011).

51. Li, H. Aligning sequence reads, clone sequences and assembly contigs with BWA-MEM. Preprint at https://arxiv.org/abs/1303.3997 (2013).

52. McKenna, A. *et al.* The Genome Analysis Toolkit: a MapReduce framework for analyzing next-generation DNA sequencing data. *Genome Res.* **20,** 1297–1303 (2010).

53. Quinlan, A. R. & Hall, I. M. BEDTools: a flexible suite of utilities for comparing genomic features. *Bioinformatics* **26,** 841–842 (2010).

54. Li, H. *et al.* The Sequence Alignment/Map format and SAMtools. *Bioinformatics* **25,** 2078–2079 (2009).

55. Zafar, H., Wang, Y., Nakhleh, L., Navin, N. & Chen, K. Monovar: single-nucleotide variant detection in single cells. *Nat. Methods* **13,** 505–507 (2016).

56. R Core Team. R: A Language and Environment for Statistical Computing. (2017).

57. Sestelo, M., Villanueva, N. M., Meira-Machado, L. & Roca-Pardiñas, J. FWDselect: An R Package for Variable Selection in Regression Models. *The R Journal* **8,** (2016).
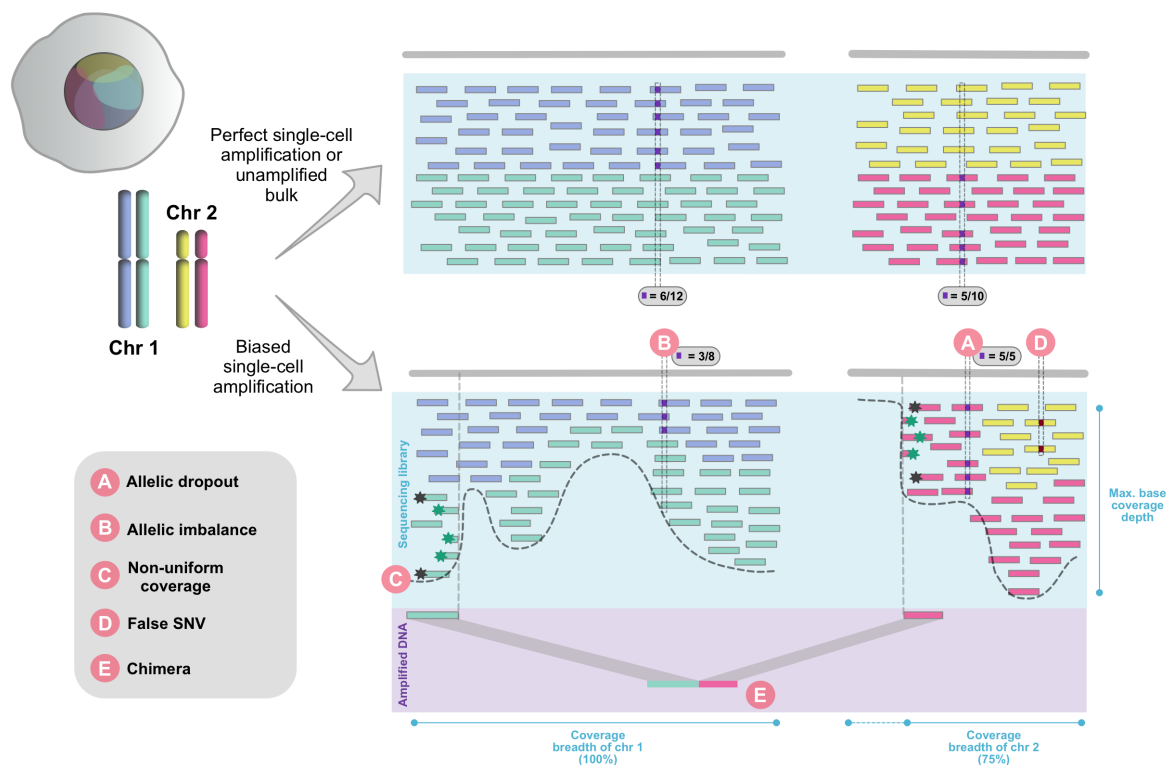
Fig. 1 | scWGA technical errors. On top, there is a representation of reads from a sequencing library constructed from perfectly amplified single-cell DNA material or, commonly, unamplified bulk. Reads coming from a sequencing library built from the product of a biased amplification are shown at the bottom. Single-cell amplification starts from a single pair of homologous chromosomes (Chr 1 and 2) while the unamplified bulk library is directly constructed from lots of chromosome pairs. During the amplification, which originated the second sequencing library, several biases occurred. On the one hand, some templates were not amplified at all (A: allelic dropout), or they were not copied as many times as their homologous sequences leading to a disproportion of maternal and paternal alleles (B: allelic imbalance). The latter contributes (although is not strictly required) to the coverage non-uniformity across the genome (C: Non-uniform coverage). The uneven coverage results in a decrease of the coverage breadth (proportion of genome covered by at least 1 read). On the other hand, during the amplification the DNA polymerase introduced a single-nucleotide variant not present in the original template (D: false SNV) as well as one chimeric amplicon (E: chimera), due to a replication error and a strand displacement, respectively. Discordant paired-end reads (grey stars) and split reads (green stars) reveal the presence of such chimeric amplicons. Little squares represent alternate alleles at original true germline sites (A,B) and one false SNV (D). Although amplicons are usually longer than reads, here they have been shortened to facilitate the representation.
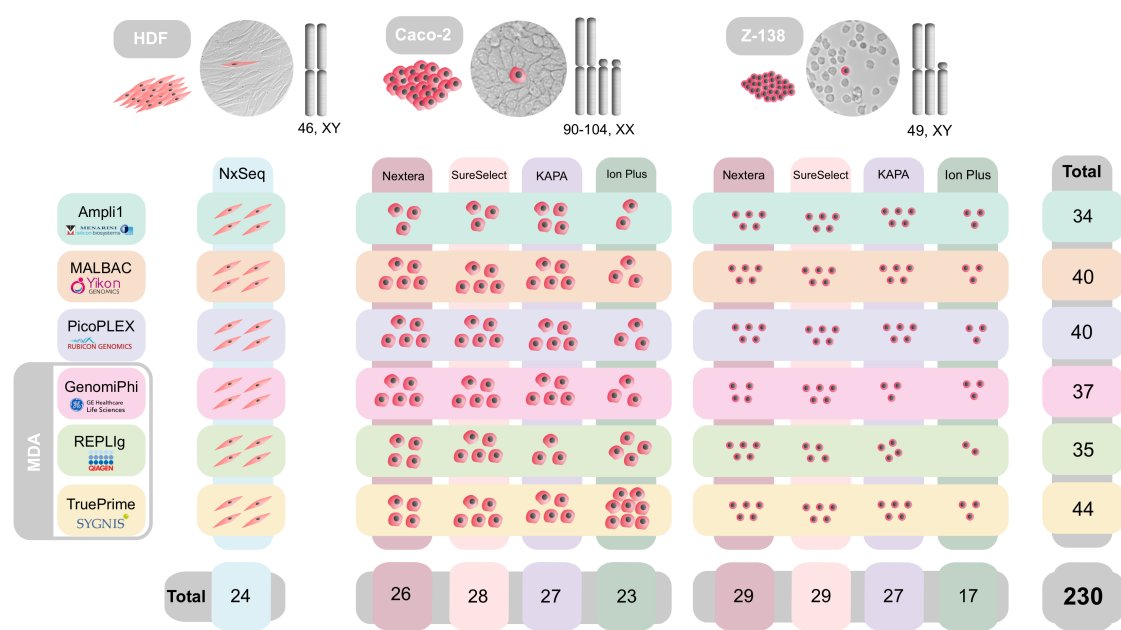
19

Fig. 2 | Experimental design. 24 HDF single-cells, 104 Caco-2 single-cells and 102 Z-138 single-cells sorted by FACS were amplified using six scWGA methods (three MDA and three non-MDA). Sequencing libraries were constructed following four different protocols for Caco-2 and Z-138 and one for HDF. A bulk sample from the HDF cell line was also extracted and sequenced as unamplified control.
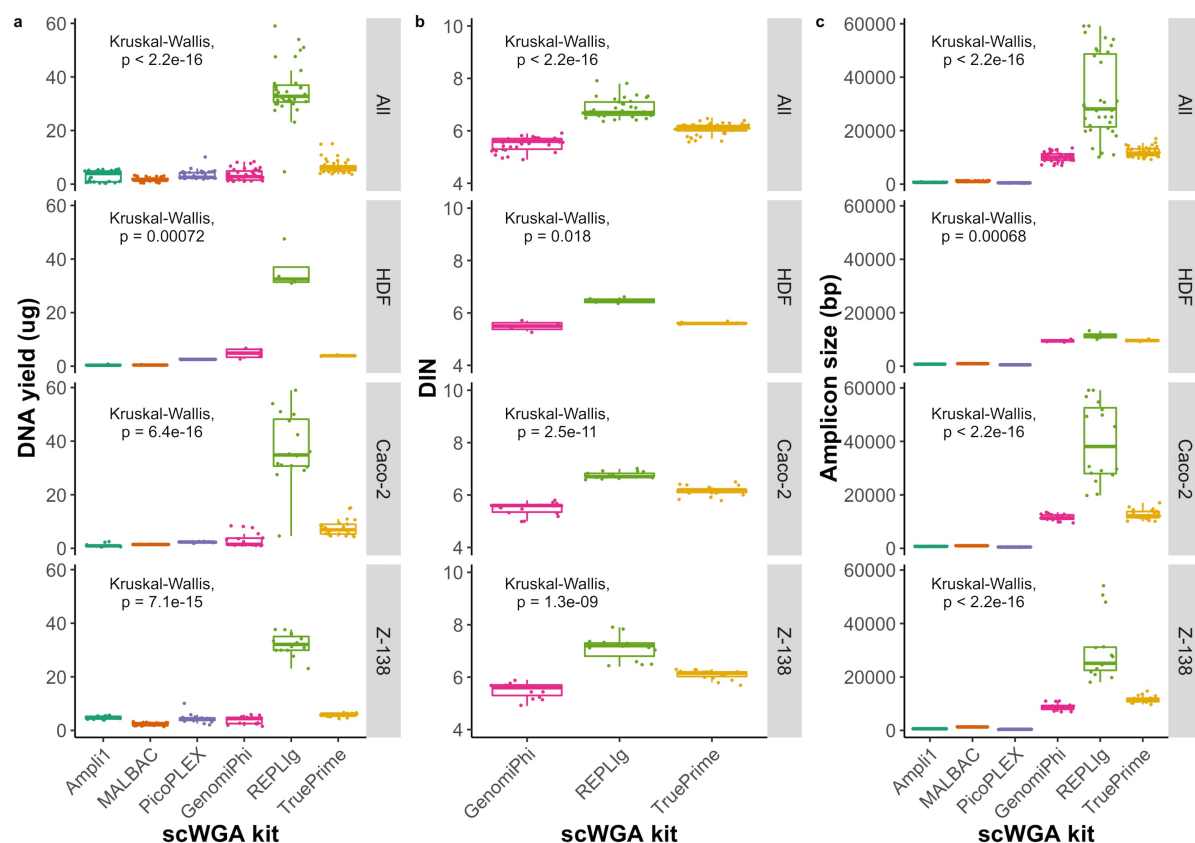
Fig. 3 | Amplification yield. a, DNA yield. **b,** DIN values (only MDA methods were measured). **c,** Amplicon size. Results are also shown combining the three cell lines (All). **a-c,** Boxplots: the central line indicates the median, while the box limits correspond to the Q1 and Q3 quartiles; upper and lower whiskers extend from Q3 to Q3 + 1.5 × (Q3 - Q1) and from Q1 to Q1 - 1.5 × (Q3-Q1), respectively. Kruskal-Wallis test p-values are shown for each dataset.
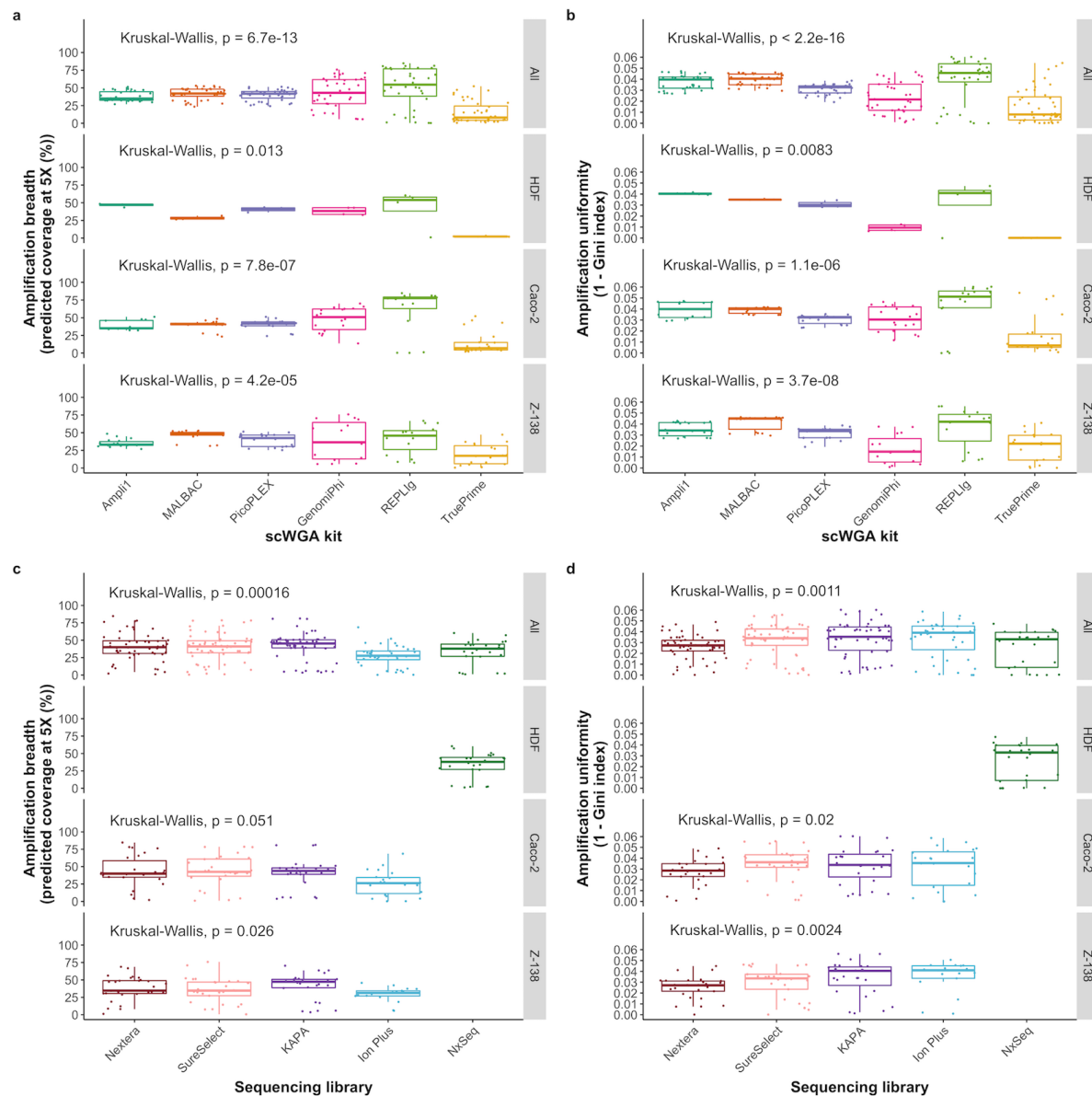
Fig. 4 | Amplification breadth and uniformity. a,b, Effect of the scWGA method on (**a**) predicted amplification breadth, measured by the percentage of the genome predicted to be covered at 5X, and (**b**) amplification uniformity, measured as 1 minus the Gini index of the resulting Lorenz curves, for the different scWGA kits. **c,d,** Effect of the sequencing library on (**c**) predicted amplification breadth and (**d**) amplification uniformity. **a-d,** Boxplots: the central line indicates the median, while the box limits correspond to the Q1 and Q3 quartiles; upper and lower whiskers extend from Q3 to Q3 + 1.5 × (Q3 - Q1) and from Q1 to Q1 - 1.5 × (Q3-Q1), respectively. Kruskal-Wallis test p-values are shown.
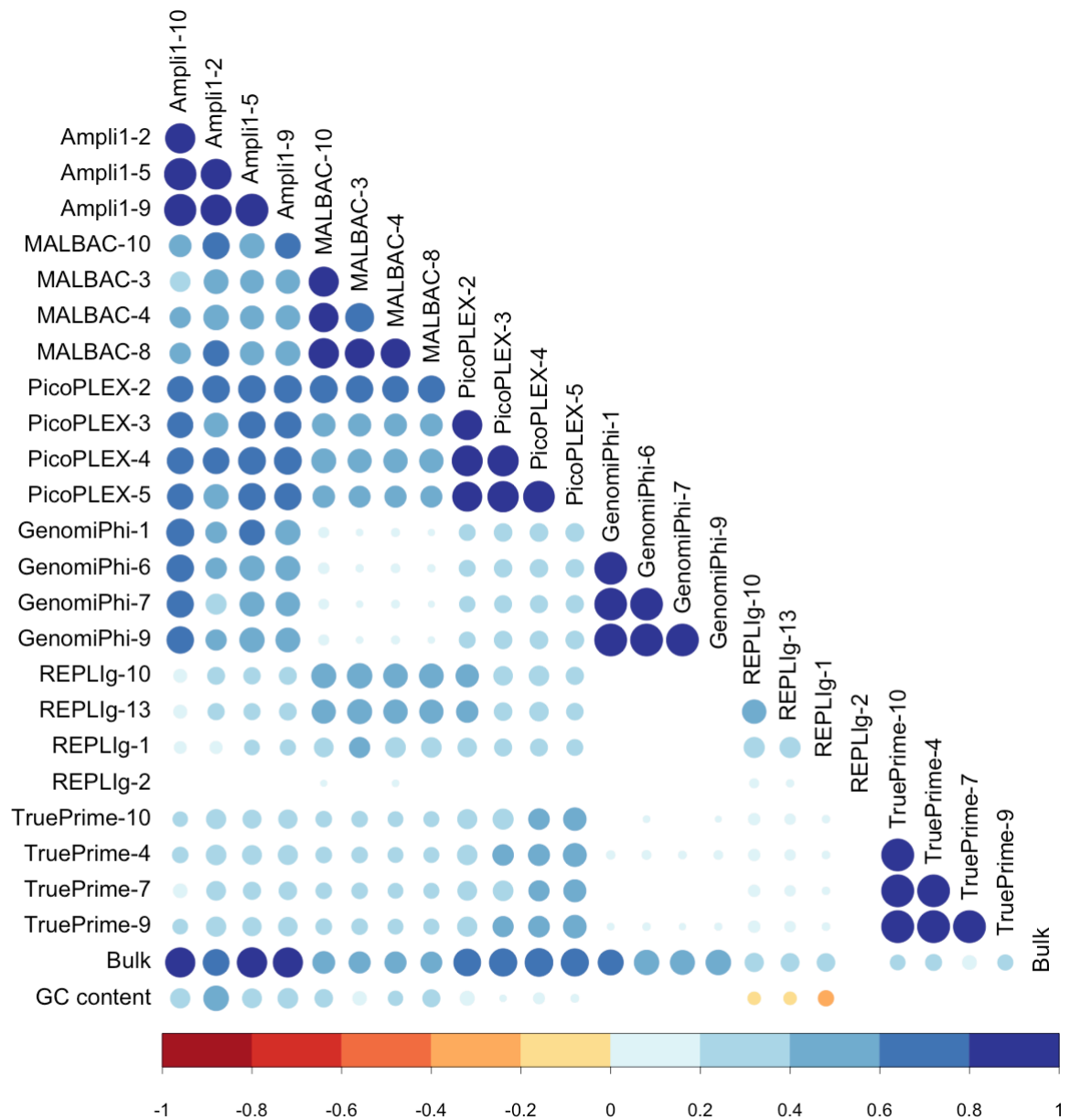
Fig. 5 | Amplification recurrence. Correlation plot of read counts along 1 Mb-long genome windows**.** The size of the dots indicates the Pearson correlation coefficient value from low (small) to high (big) and colored differently if positive (blue scale) or negative (red scale). Only statistically significant values (p-value < 0.05) are shown.
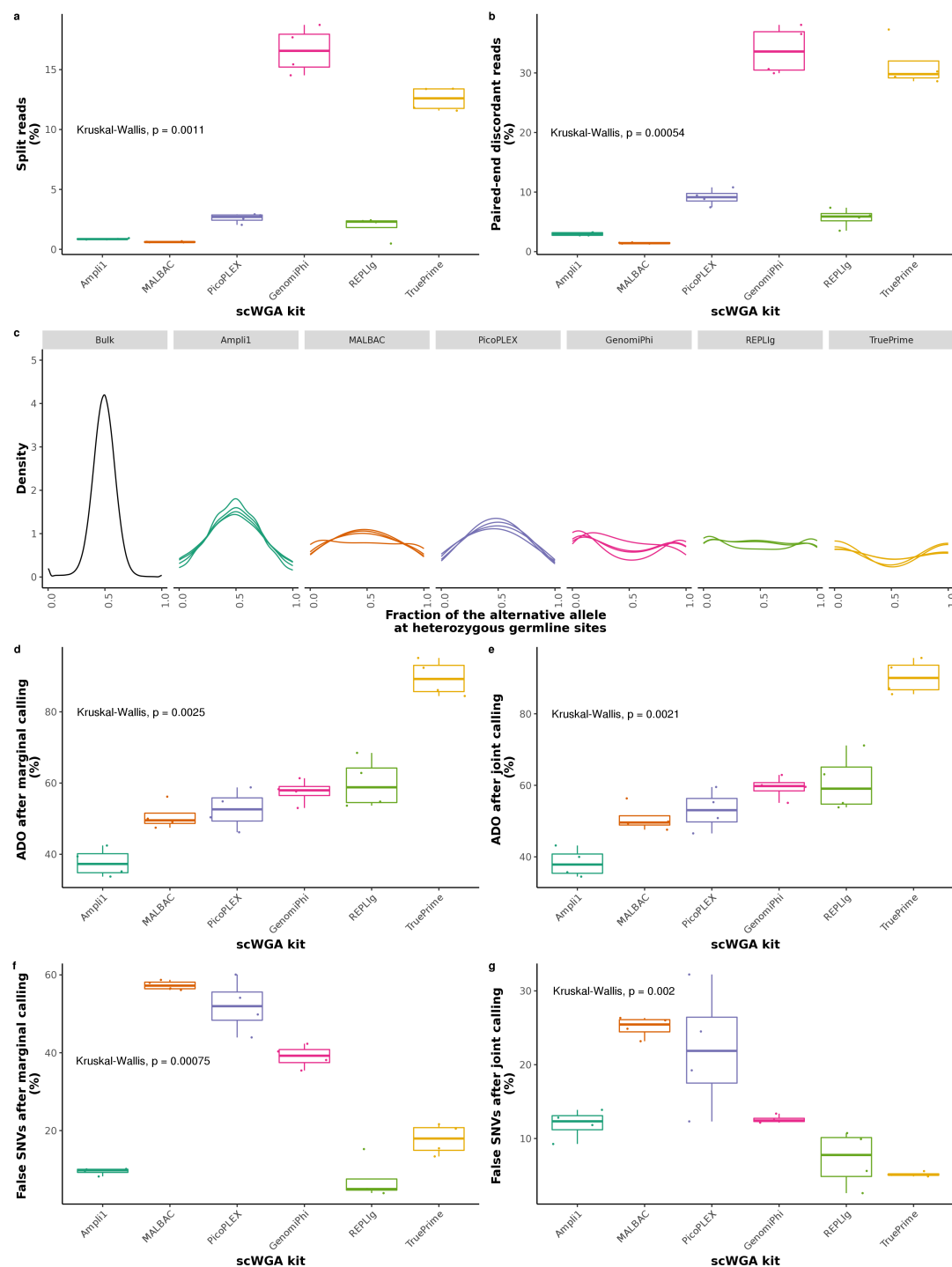
Fig. 6 | Chimera rates, allelic imbalance, ADO and false SNV calls. a-g, all these values were measured from the healthy cell line HDF. **a**, paired-end discordant reads. **b,** split reads. **c**, Kernel density estimation of the alternative allele fraction at heterozygous germline sites. Each line within a panel tab represents a different single-cell. For the density estimation we used all the positions called as heterozygous in the bulk with *HaplotypeCaller* and with at least 6 reads of coverage in the single-cells. The density of one of the REPLIg single-cell is not shown as it only had 7 positions with more than 5 reads, too few to obtain a smooth distribution of the allele fraction. **d**, ADO calculated after marginal genotype calling. **e**, ADO calculated after joint genotype calling. **f,** False SNVs calculated after marginal genotype calling. **g,** False SNVs calculated after joint genotype calling. **d-g,** Boxplots: the central line indicates the median, while the box limits correspond to the Q1 and Q3 quartiles; upper and lower whiskers extend from Q3 to Q3 + 1.5 × (Q3 - Q1) and from Q1 to Q1 - 1.5 × (Q3-Q1), respectively.